

## Evidence for convergence of distributed cortical processing in band-like functional zones in human entorhinal cortex

### Highlights

- Human entorhinal cortex (ERC) is organized into three parallel band-like zones
- Functionally distinct cortical networks associate with distinct ERC bands
- Different longitudinal parts of the hippocampus associate with distinct ERC bands
- Human ERC is a major convergence hub of distributed cortical processing

### Authors

Daniel Reznik, Daniel S. Margulies, Menno P. Witter, Christian F. Doeller

### Correspondence

reznikda@gmail.com

### In brief

Using precision neuroimaging, Reznik et al. discover that the human entorhinal cortex is organized into three band-like zones running in parallel to the collateral sulcus. Consistent with animal anatomy, these entorhinal cortex bands associate with functionally distinct cortical networks and different parts of the hippocampus long axis.



## Article

# Evidence for convergence of distributed cortical processing in band-like functional zones in human entorhinal cortex

Daniel Reznik,<sup>1,5,6,\*</sup> Daniel S. Margulies,<sup>2,3</sup> Menno P. Witter,<sup>4</sup> and Christian F. Doeller<sup>1,4</sup><sup>1</sup>Department of Psychology, Max Planck Institute for Human Cognitive and Brain Sciences, Leipzig 04103, Germany<sup>2</sup>Integrative Neuroscience and Cognition Center, Centre National de la Recherche Scientifique (CNRS) and Université de Paris, 75016 Paris, France<sup>3</sup>Wellcome Centre for Integrative Neuroimaging, Nuffield Department of Clinical Neurosciences, University of Oxford, Oxford OX3 9DU, UK<sup>4</sup>Kavli Institute for Systems Neuroscience, the Egil and Pauline Braathen and Fred Kavli Centre for Cortical Microcircuits, Jebsen Centre for Alzheimer's Disease, NTNU Norwegian University of Science and Technology, 7034 Trondheim, Norway<sup>5</sup>X (formerly Twitter): @reznikdan<sup>6</sup>Lead contact

\*Correspondence: reznikda@gmail.com

<https://doi.org/10.1016/j.cub.2024.10.020>**SUMMARY**

The wide array of cognitive functions associated with the hippocampus is supported through interactions with the cerebral cortex. However, most of the direct cortical input to the hippocampus originates in the entorhinal cortex, forming the hippocampal-entorhinal system. In humans, the role of the entorhinal cortex in mediating hippocampal-cortical interactions remains unknown. In this study, we used precision neuroimaging to examine the distributed cortical anatomy associated with the human hippocampal-entorhinal system. Consistent with animal anatomy, our results associate different subregions of the entorhinal cortex with different parts of the hippocampus long axis. Furthermore, we find that the entorhinal cortex comprises three band-like zones that are associated with functionally distinct cortical networks. Importantly, the entorhinal cortex bands traverse the proposed human homologs of rodent lateral and medial entorhinal cortices. Finally, we show that the entorhinal cortex is a major convergence area of distributed cortical processing and that the topography of cortical networks associated with the anterior medial temporal lobe mirrors the macroscale structure of high-order cortical processing.

**INTRODUCTION**

The entorhinal cortex and the hippocampus are critically involved in episodic memory, spatial navigation, and learning. Tract tracing studies in rodents and non-human primates indicate that the entorhinal cortex is a major gateway between the hippocampus and the neocortex.<sup>1,2</sup> The entorhinal cortex receives direct input from the perirhinal and parahippocampal cortex (postrhinal cortex in the rodent), as well as from multiple distributed regions across the broader neocortex, such as the retrosplenial, inferior parietal, and frontal cortex.<sup>3,4</sup> Because direct cortical input to the hippocampus involves mostly input to the CA1/subiculum border,<sup>5</sup> the entorhinal cortex serves as the main input source to the hippocampus and provides it with highly processed information.<sup>2</sup>

Anatomical studies examining the intrinsic connectivity within the hippocampal system in non-human primates point to at least two topographically organized gradients in connectivity between the entorhinal cortex and the hippocampus. One connectivity gradient relates the anterolateral to posteromedial position in the entorhinal cortex to the transverse position in CA1 and subiculum, such that more anterolateral parts of the entorhinal cortex are connected to distal parts of CA1 (further away from CA3)

and proximal parts of subiculum (further away from pre/parasubiculum), and more posteromedial parts of the entorhinal cortex are connected with proximal parts of CA1 (closer to CA3) and distal parts of subiculum (closer to pre/parasubiculum).<sup>6</sup> An additional connectivity gradient relates the medial-lateral axis of the entorhinal cortex with the longitudinal axis of the hippocampus, such that medially situated portions of the entorhinal cortex that are closer to the hippocampus are connected with the anterior hippocampus, and more lateral portions of the entorhinal cortex that are closer to the rhinal sulcus (the sulcus delimiting the entorhinal cortex in rodents and non-human primates) are connected with the posterior hippocampus.<sup>6,7</sup> Similar connectivity gradients have also been observed in rodents,<sup>8,9</sup> cats,<sup>10</sup> and bats,<sup>11</sup> suggesting potentially conserved entorhinal-hippocampal connectivity patterns across the mammalian lineage.

Importantly, different portions of the entorhinal cortex can be also characterized by heterogeneous anatomical input from the neocortex.<sup>3,12</sup> While this is especially true for anterolateral and posteromedial parts of the entorhinal cortex, different parts of the entorhinal medial-lateral axis receive different cortical input as well.<sup>12,13</sup> Therefore, together with the topographical connectivity gradients between the entorhinal cortex and the



hippocampus, differences in the type of cortical input to different parts of the entorhinal cortex impose important anatomical constraints on information processing and hint to functional differentiations within the hippocampal-entorhinal system.<sup>14,15</sup>

In humans, multiple studies explored the functional properties of the entorhinal cortex and the hippocampus. Despite the challenges in functional magnetic resonance imaging (fMRI) of the anterior medial temporal lobe (MTL), several studies have consistently demonstrated a functional dissociation within the entorhinal cortex. Whereas the anterolateral part of the entorhinal cortex was found to be preferably involved in processing external information, such as temporal sequence and object-related information, the more posteromedial part was found to be preferably involved in processing spatial information.<sup>16–22</sup> Furthermore, using fMRI connectivity as a proxy for anatomical connectivity,<sup>23,24</sup> it was found that the anterolateral and posteromedial parts of the human entorhinal cortex are associated with different parts of the subiculum and with distinct cortical systems supporting different aspects of mnemonic processing.<sup>25–28</sup>

In contrast to the entorhinal cortex, previous research into the functional properties of the human hippocampus is more abundant. These observations point to several functional and structural dissociations along the hippocampal longitudinal axis.<sup>14,29,30</sup> Consistent with fine-scale spatial representations in the rodent dorsal hippocampus,<sup>31</sup> the human posterior hippocampus was found to be engaged during detailed spatial processing and retrieval of detailed autobiographical memories.<sup>32–34</sup> Human anterior hippocampus, on the other hand, was found to be associated with general, gist-like memories, in line with more coarse spatial representations in the rodent ventral hippocampus.<sup>34,35</sup> At the level of hippocampal interactions with the broader neocortex, important recent observations used individualized task-based and connectivity-based methods<sup>36–39</sup> to demonstrate that different parts of the human hippocampus are associated with different distributed cortical networks.<sup>40,41</sup> Specifically, while the anterior hippocampus was reported to be associated with one subdivision of the canonical default network, default network A (DN-A),<sup>39</sup> the posterior hippocampus was reported to be associated with the parietal memory network, known also as the salience network (PMN/SAL).<sup>42–44</sup>

In this study, we aimed to extend these findings and to explore the cortical networks linked to the entorhinal cortex to complement our understanding of the distributed cortical processing associated with the hippocampal-entorhinal system in humans. Using precision fMRI data specifically optimized for high-quality signal in the MTL, we previously discovered that parts of human entorhinal cortex are associated with default network B (DN-B), and parts of the pre/parasubiculum are associated with DN-A.<sup>37</sup> Our prior results pointed to potentially additional cortical networks associated with the intraparietal sulcus that are linked to the most lateral parts of the entorhinal cortex.<sup>37</sup> Therefore, in this study, in addition to examining entorhinal cortex associations with cortical networks DN-A and DN-B, we considered networks with known representations in the intraparietal sulcus—the cortical network PMN/SAL<sup>44,45</sup> and two subdivisions of the canonical frontoparietal network<sup>46</sup>—frontoparietal network A (FPN-A) and frontoparietal network B (FPN-B).<sup>42,47</sup> We leveraged whole-brain individualized network architecture to explore in detail cortical networks that are associated with subregions of

the human entorhinal cortex and the hippocampus. Using two independent datasets for networks definition and for exploring associations with the entorhinal cortex and the hippocampus, we discovered consistent representations of at least four distributed cortical networks associated with the human hippocampal-entorhinal system.

## RESULTS

In this study, we analyzed fixation task data (resting state) from four densely sampled individuals collected using 7T fMRI.<sup>37</sup> We leveraged whole-brain individualized network architecture and unprecedentedly high-quality signals in the MTL to explore the distributed cortical anatomy associated with the human hippocampal-entorhinal system. More specifically, in each participant, we used two independent datasets—a network estimation dataset and an exploration dataset. Network estimation datasets were used to identify five participant-specific cortical networks of interest—DN-A, DN-B, FPN-A, FPN-B, and PMN/SAL (Figures 1 and S1). After defining the cortical networks of interest, independent exploration datasets were used to estimate network-level associations with the entorhinal cortex and the hippocampus.

### Distinct cortical networks are associated with the entorhinal cortex in a band-like fashion

Using independent exploration datasets, we found that the cortical network DN-A was associated with voxels located in the most medial parts of the parahippocampal gyrus, anatomically corresponding to the pre/parasubiculum, the entorhinal cortex, and to the transitional area between the pre/parasubiculum and the entorhinal cortex,<sup>48,49</sup> (Figure 2, red; see discussion). The cortical network DN-A was associated with the entire longitudinal extent of the anterior part of the parahippocampal gyrus with robust representations both in the posterior and anterior entorhinal cortex, including the ambient gyrus<sup>50</sup> and pre/parasubiculum.

In contrast, we found that the cortical network DN-B was associated with voxels located in the more laterally situated portions of the parahippocampal gyrus, anatomically corresponding to the entorhinal cortex but closer to the collateral sulcus than the area associated with DN-A (Figure 2, yellow). Similar to DN-A, the cortical network DN-B was associated with the entire longitudinal axis of the anterior part of the parahippocampal gyrus with robust representations both in the posterior entorhinal cortex and anterior entorhinal cortex including the ambient gyrus.

Finally, we found that voxels located in the most lateral parts of the parahippocampal gyrus, anatomically corresponding to the entorhinal cortex delimited by the collateral sulcus, were associated with two distributed cortical networks—PMN/SAL and FPN-B. Importantly, while the cortical network PMN/SAL was consistently associated with voxels in the anterior part of the entorhinal cortex (Figure 2, blue), the cortical network FPN-B was associated with voxels in the posterior part of the entorhinal cortex (Figure 2, cyan). No consistent voxels associated with the cortical network FPN-A were observed in the entorhinal cortex. However, we observed voxels consistently associated with this cortical network located deep within the collateral sulcus, anatomically corresponding to the anterior parts of the perirhinal cortex (Figure S2).

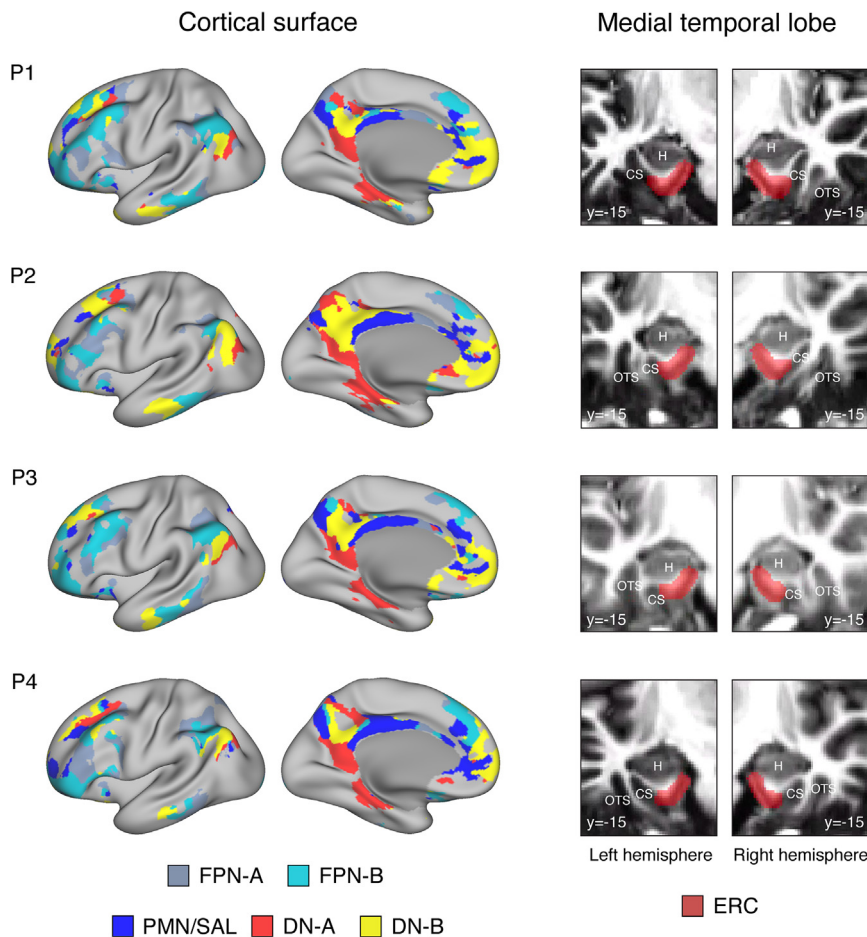


**Figure 1. Individually defined cortical networks of interest and one exemplar level of entorhinal cortex mask**

Using network estimation datasets, we applied multi-session hierarchical Bayesian modeling to define five cortical networks of interest in each participant (P1–P4; left). Following our prior results,<sup>37</sup> we considered cortical networks associated with the inferior parietal lobe and the intra-parietal sulcus. DN-A, default network A; DN-B, default network B; FPN-A, frontoparietal network A; FPN-B, frontoparietal network B; PMN/SAL, parietal memory network/salience network. The network labels are repeated in other figures throughout the manuscript. Next, we defined the entorhinal cortex masks for each participant (right). Note that the masks covered the entire parahippocampal gyrus and therefore included the entorhinal cortex and at least parts of the pre/parasubiculum (see Figure S1 for masks covering the anterior entorhinal cortex). CS, collateral sulcus; ERC, entorhinal cortex; H, hippocampus; OTS, occipitotemporal sulcus.

hippocampus, were with the posteromedial cortex and inferior parietal lobe. The strongest connections associated with the posterior part of the entorhinal cortex closest to the collateral sulcus and with the intermediate part of the entorhinal cortex were more distributed across the cortical mantle and included the lateral surface of the temporal lobe, posteromedial cortex, parietal cortex, and frontal cortex.

To conclude, we found that the human entorhinal cortex is organized into three

band-like zones that follow the entire longitudinal extend of the entorhinal cortex. The most medial band was found to be associated with the cortical network DN-A, the intermediate band was found to be associated with DN-B, and the lateral band was found to be associated with PMN/SAL and FPN-B (see Figure 5A for summary and Figure 5B for the entorhinal cortex two-dimensional surface map).

To validate that distinct parts of the entorhinal cortex are preferably associated with each of the cortical networks, we calculated Fisher z-transformed Pearson correlation coefficients associating the subregions of the entorhinal cortex with the time series of each vertex in the cortical surface without imposing any network restrictions, allowing them to correlate with all cortical vertices.<sup>40,51</sup> As can be seen from Figure S3, correlations of different parts of the entorhinal cortex with the broader neocortex showed spatial connectivity patterns that fell within the network-specific boundaries in each individual (defined using the network estimation datasets). Moreover, formal analyses showed greatest Fisher z-transformed Pearson correlation coefficients between the time series derived from subregions of the entorhinal cortex and the time series of the corresponding networks of interest compared with the time series of other networks (Figure S4; paired t tests, all  $p < 0.05$ ).

Next, we thresholded the Fisher z-transformed Pearson correlation coefficients associating the subregions of the entorhinal cortex with the cortical surface to identify the cortical regions that display the strongest connectivity patterns with different subregions of the entorhinal cortex. We found that the strongest connections of the anterior part of the entorhinal cortex closest to the collateral sulcus were with frontal cortical regions, such as the orbitofrontal cortex and medial prefrontal cortex. The strongest connections of the medial part of the entorhinal cortex, closest to the

hippocampus, were with the posteromedial cortex and inferior parietal lobe. The strongest connections associated with the posterior part of the entorhinal cortex closest to the collateral sulcus and with the intermediate part of the entorhinal cortex were more distributed across the cortical mantle and included the lateral surface of the temporal lobe, posteromedial cortex, parietal cortex, and frontal cortex.

### Distinct cortical networks are associated with the hippocampus

Given the animal tract-tracing data indicating strong direct anatomical connectivity between the entorhinal cortex and the hippocampus, we explored how the cortical networks we found to be associated with the entorhinal cortex are related to the hippocampus. First, we sought to replicate previous reports indicating that different parts of the hippocampal longitudinal axis are associated with distinct cortical regions.<sup>40,41</sup> Using independent exploration datasets, consistent with prior studies, we found that the cortical network DN-A is associated with voxels located preferably in the anterior hippocampus, and the cortical network PMN/SAL is associated with voxels located preferably in the posterior hippocampus.

Next, we explored hippocampal associations separately with each of the cortical networks DN-A, DN-B, PMN/SAL, and FPN-B. In agreement with the winner-takes-all approach, we



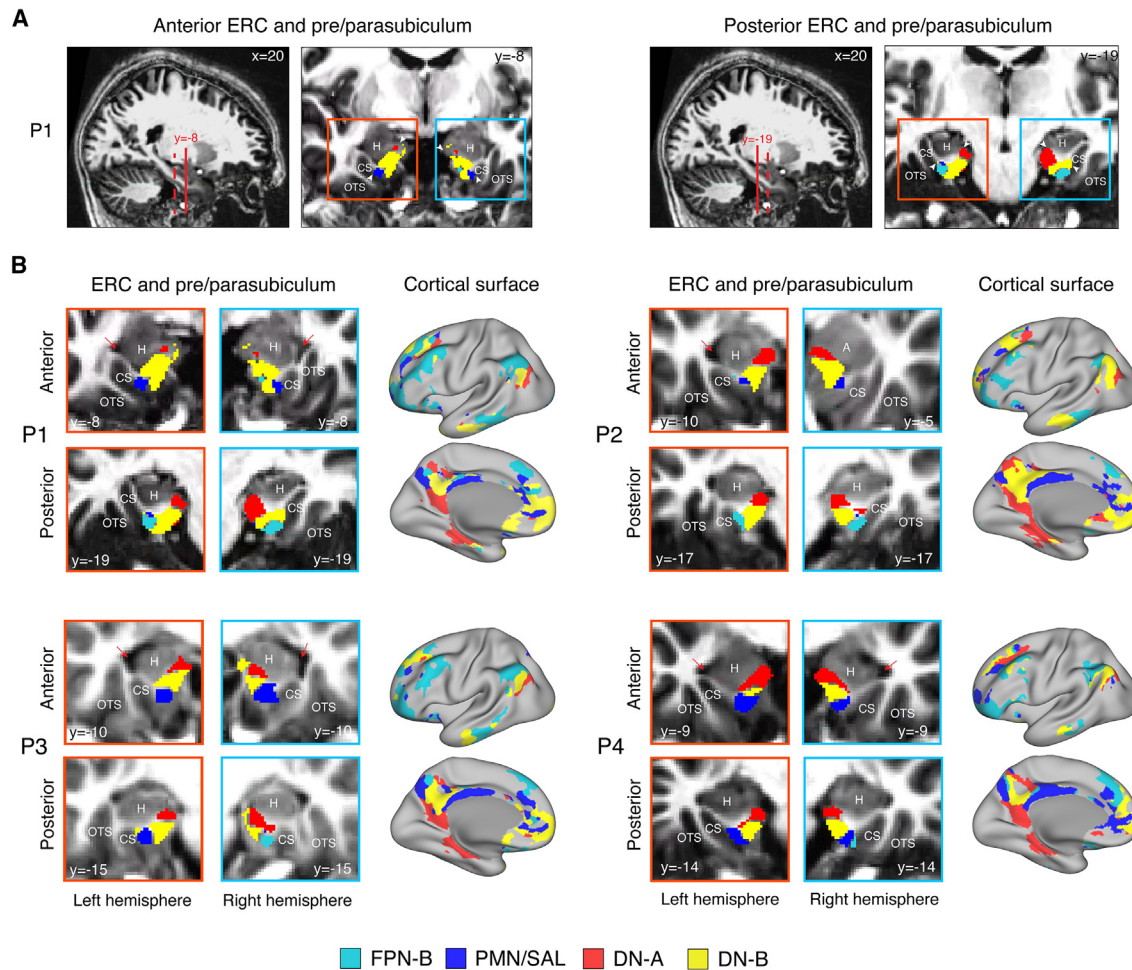


**Figure 2. Cortical networks associated with the entorhinal cortex are organized into three parallel bands**

(A) Anatomical locations of anterior and posterior entorhinal cortex slices presenting winner-takes-all results from one representative participant (P1). Note that the cyan box represents the left hemisphere, and the orange box represents the right hemisphere. White arrowheads mark the borders of the parahippocampal gyrus.

(B) Using independent exploration datasets and the winner-takes-all approach, we found that the entorhinal cortex is associated with at least four distributed cortical networks across all participants—FPN-B, PMN/SAL, DN-B, and DN-A. Cortical networks FPN-B and PMN/SAL (cyan and blue) are associated with the most lateral parts of the entorhinal cortex, closest to the collateral sulcus. More intermediate parts of the entorhinal cortex are associated with the cortical network DN-B (yellow). The most medial parts of the entorhinal cortex, closest to the hippocampus, are associated with the cortical network DN-A (red; see [discussion](#)). The cortical network PMN/SAL is associated with the anterior parts of the entorhinal cortex in all four participants, but in two participants (P3 and P4) it also extends to the posterior parts of the entorhinal cortex. Note the band-like organization of the entorhinal cortex with DN-A being the medial band, DN-B the intermediate band, and PMN/SAL and FPN-B the lateral band. For each participant, the right side of the figure displays the cortical networks of interest on the cortical surface, and the left side of the figure displays corresponding associations with the anterior and posterior entorhinal cortex presented on representative coronal slices in right and left hemisphere. Red arrows in the anterior entorhinal cortex slices point to the beginning of the temporal horn of the lateral ventricle serving as the main landmark for identifying the ambient gyrus. A, amygdala; CS, collateral sulcus; ERC, entorhinal cortex; H, hippocampus; OTS, occipito-temporal sulcus.

See also [Figures S2–S4](#).

found consistent associations of the cortical networks PMN/SAL and DN-A with the posterior and anterior hippocampus, respectively. Furthermore, we found that the cortical network DN-B was consistently associated with voxels located in the anterior hippocampus ([Figure 3](#)). Because the cortical network DN-B was associated with the entorhinal cortex intermediate band, situated between the parts of entorhinal cortex associated with the cortical networks DN-A (medial band) and PMN/SAL (lateral band), we hypothesized that the cortical network DN-B might be

associated with the intermediate hippocampus, located between its anterior and posterior parts.<sup>52</sup> However, the hippocampal voxels associated with the cortical network DN-B were largely overlapping with the hippocampal voxels associated with the cortical network DN-A, and we could not identify consistent anatomical dissociations between these two networks within the hippocampus using our dataset. No anatomically consistent connectivity patterns between the cortical network FPN-B and the hippocampus were observed.

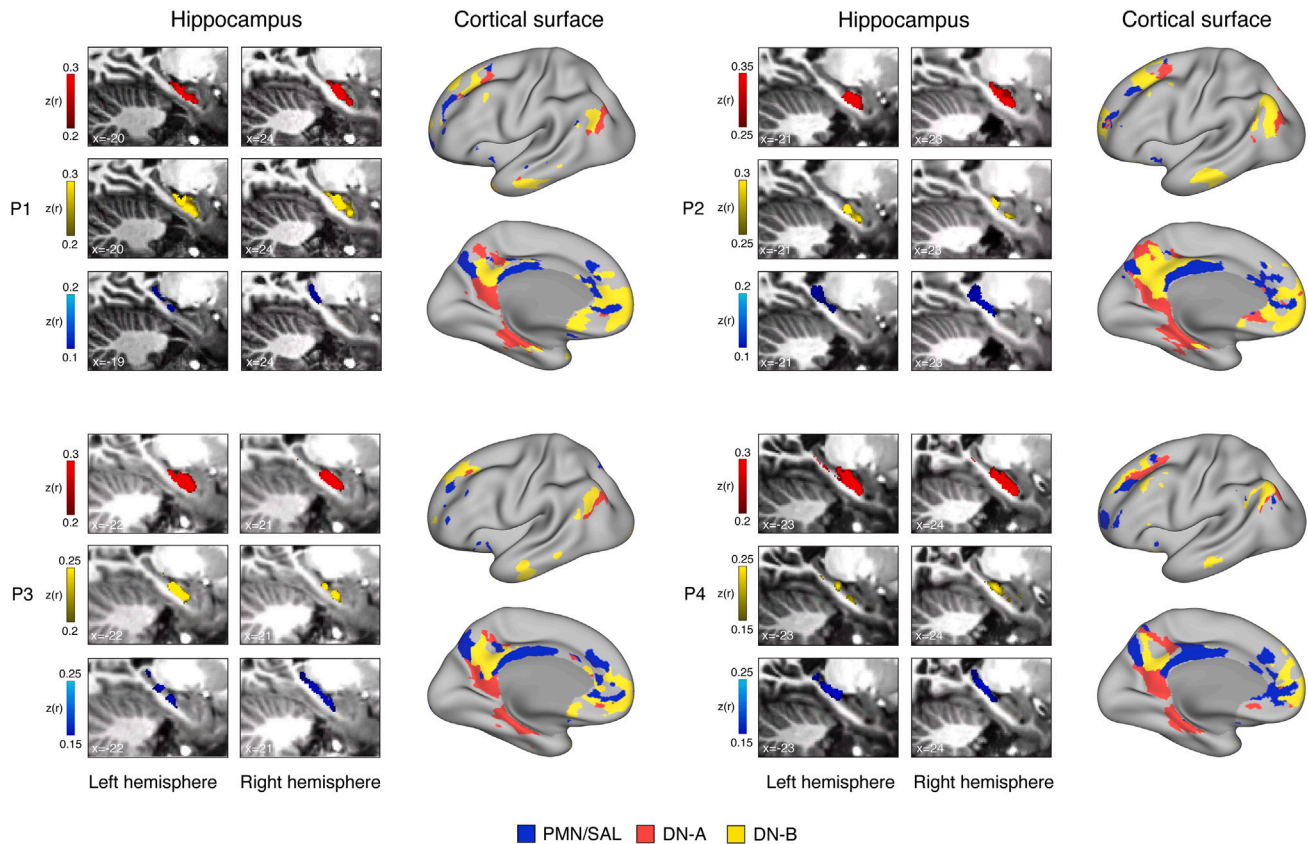


**Figure 3. Cortical networks associated with the hippocampal longitudinal axis**

Using independent exploration datasets, we demonstrate that in all four participants, the cortical network PMN/SAL (blue) is preferably associated with the posterior hippocampus. The cortical networks DN-A (red) and DN-B (yellow) are associated with the anterior hippocampus. Despite having a strong anatomical prior based on animal tract tracing data, we could not dissociate the cortical networks DN-A and DN-B in the hippocampus (see [discussion](#)). For each participant, the right side of the figure displays the cortical networks of interest on the cortical surface, and the left side of the figure displays corresponding associations with the hippocampus presented on representative sagittal slices in right and left hemispheres. Note that the hippocampal masks included the subiculum, but not the pre/parasubiculum.

### Convergence of distributed cortical processing in the human hippocampal-entorhinal system

Animal anatomical studies indicate that the entorhinal cortex is a main cortical convergence area in the hippocampal memory system.<sup>2,53</sup> Since we found that the human hippocampal-entorhinal system is associated with at least four distributed cortical networks, we wished to examine to what degree cortical hierarchical processing<sup>54</sup> convergences on the hippocampal-entorhinal system compared with other subregions of the MTL—the perirhinal cortex and the parahippocampal cortex. To this end, we calculated a low-dimensional embedding from whole-brain connectivity data (see [STAR Methods](#) for more details) and visualized its principal gradient on each participant’s cortical surface ([Figure 4](#)). We interpreted the principal gradient values as a relative position on the unimodal-transmodal processing axis.<sup>55</sup> Even with complex areal topography observed at the individual-subject level,<sup>56</sup> our results indicate that the macroscale spatial distribution of the principal gradient closely follows previously reported group-level topography (compare to Margulies et al.<sup>55</sup>). More specifically, the lowest principal gradient values were observed in anatomical locations corresponding to the primary somato-motor cortex, primary auditory cortex, and primary visual cortex, and the highest principal gradient values were observed in the inferior parietal

lobule, lateral surface of the temporal lobe, posteromedial cortex, MTL, and frontal cortex. These findings indicate that diffusion embedding can be applied for robustly describing participant-specific connectivity gradients at the whole-brain level.

Next, to position the subregions of the human MTL on the principal connectivity gradient, we averaged the principal gradient values for each of the cortical networks that we found to be associated with the hippocampus, entorhinal cortex, perirhinal cortex, and parahippocampal cortex. Corresponding to our findings, the cortical networks associated with the entorhinal cortex were DN-A, DN-B, FPN-B, and PMN/SAL. The cortical networks associated with the hippocampus were DN-A, DN-B, and PMN/SAL. The cortical networks associated with the perirhinal cortex were the dorsal attention network A (dATN-A)<sup>37</sup> and FPN-A (currently a descriptive finding). The cortical networks associated with the parahippocampal cortex were DN-A and dATN-A.<sup>37</sup> For each participant, we used individualized cortical network boundaries overlaid on the participant-specific cortical distribution of the principal gradient. Our results demonstrate that within human MTL, the average principal gradient value of the cortical networks associated with the entorhinal cortex and the hippocampus was greater than that for the perirhinal cortex and the parahippocampal cortex ([Figure 4](#); see [Figure S5](#) for gradient values of each network

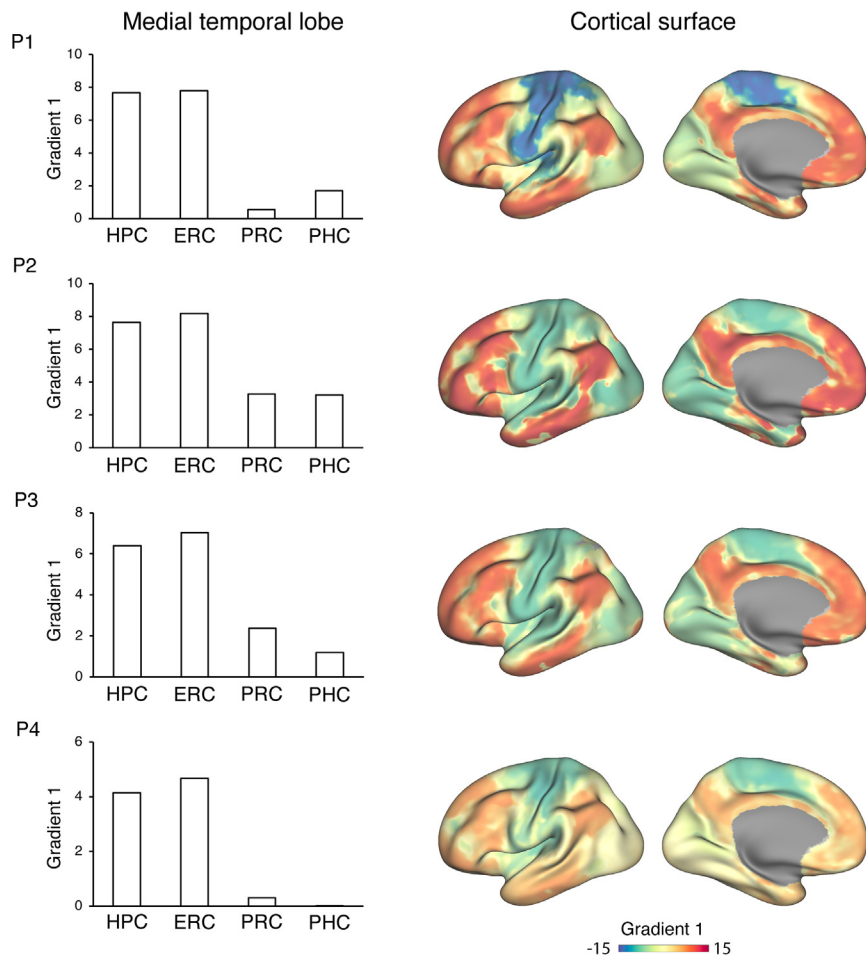


**Figure 4. Entorhinal cortex is a major cortical convergence area in human MTL**

To position the subregions of human MTL on the unimodal-transmodal processing axis, we calculated their principal gradient values from the within-participant diffusion embedding analysis. As can be seen from the diffusion embedding analysis results (right), the spatial distribution of the principal gradient in individual subjects closely follows previously reported group-level topography on the macroscale level. Next, we calculated the principal gradient values of the hippocampus, entorhinal cortex, perirhinal cortex, and parahippocampal cortex based on the principal gradient values of the cortical networks associated with each of the MTL subregions (left). In all participants, the principal gradient values of the entorhinal cortex were comparable with that of the hippocampus and higher compared with that of the perirhinal and parahippocampal cortex, suggesting a major cortical convergence role of the human hippocampal-entorhinal system. ERC, entorhinal cortex; HPC, hippocampus; PHC, parahippocampal cortex; PRC, perirhinal cortex. See also [Figure S5](#).

anterior parts of the hippocampus, and PMN/SAL associates with posterior parts of the hippocampus ([Figure 5A](#)).

#### Distributed cortical processing associated with the entorhinal cortex

We expand our previous findings<sup>37</sup> and show that the human entorhinal cortex is

associated with each of the MTL subregions). These results demonstrate that the hippocampal-entorhinal system is the main convergence area of cortical processing in the human memory system.

#### DISCUSSION

In this study, we explored distributed cortical networks associated with the human hippocampal-entorhinal system using precision fMRI data from four densely sampled individuals. Our results suggest that the human entorhinal cortex is associated with distinct cortical networks that follow the entorhinal medial-lateral and anterior-posterior axes. The entire anterior-posterior extent of the most medial part of the entorhinal cortex, situated closest to the hippocampus, is associated with the cortical network DN-A (medial band of the entorhinal cortex). The more laterally situated, intermediate part of the entorhinal cortex, over its full anterior-posterior extent, is associated with the cortical network DN-B (intermediate band of the entorhinal cortex). The most lateral part of the entorhinal cortex, delimited by the collateral sulcus, is associated with the cortical networks PMN/SAL (anterior part of the lateral band of the entorhinal cortex) and FPN-B (posterior part of the lateral band; [Figure 5](#)). Furthermore, we demonstrate that the human hippocampus is associated with distinct distributed cortical networks that follow its longitudinal axis—DN-A and DN-B associate with

associated with at least four distributed cortical networks, DN-A, DN-B, PMN/SAL, and FPN-B, which define three anterior-posteriorly running band-like zones in the entorhinal cortex. These bands are positioned in parallel along the medial-lateral axis of the entorhinal cortex. The cortical network DN-A was previously shown to be associated with the human pre/parasubiculum,<sup>37,58</sup> but not with the entorhinal cortex. In rodents, pre/parasubiculum neurons bordering the entorhinal cortex show both functional and structural similarities with entorhinal cortex neurons,<sup>48,49,59</sup> thus creating a complex transitional area between these two subregions of the hippocampal system. In monkeys, posteromedial entorhinal cortex receives direct input from the retrosplenial cortex<sup>3</sup> and parahippocampal cortex (area TH),<sup>7</sup> which are associated with the cortical network DN-A in humans.<sup>37</sup> Despite these connectivity data, in addition to the entorhinal cortex, anatomical projections from the retrosplenial cortex and the parahippocampal area TH target the pre/parasubiculum as well, thus making it challenging to attribute the cortical network DN-A to either the pre/parasubiculum or the entorhinal cortex. Nevertheless, our current analyses allowed us to discover consistent associations of the cortical network DN-A with the anterior parts of the MTL around and including the ambient gyrus ([Figures 2 and 5B](#)). Cytoarchitectonic analysis of the human ambient gyrus showed that it is largely formed by the entorhinal cortex, specifically by its medial intermediate



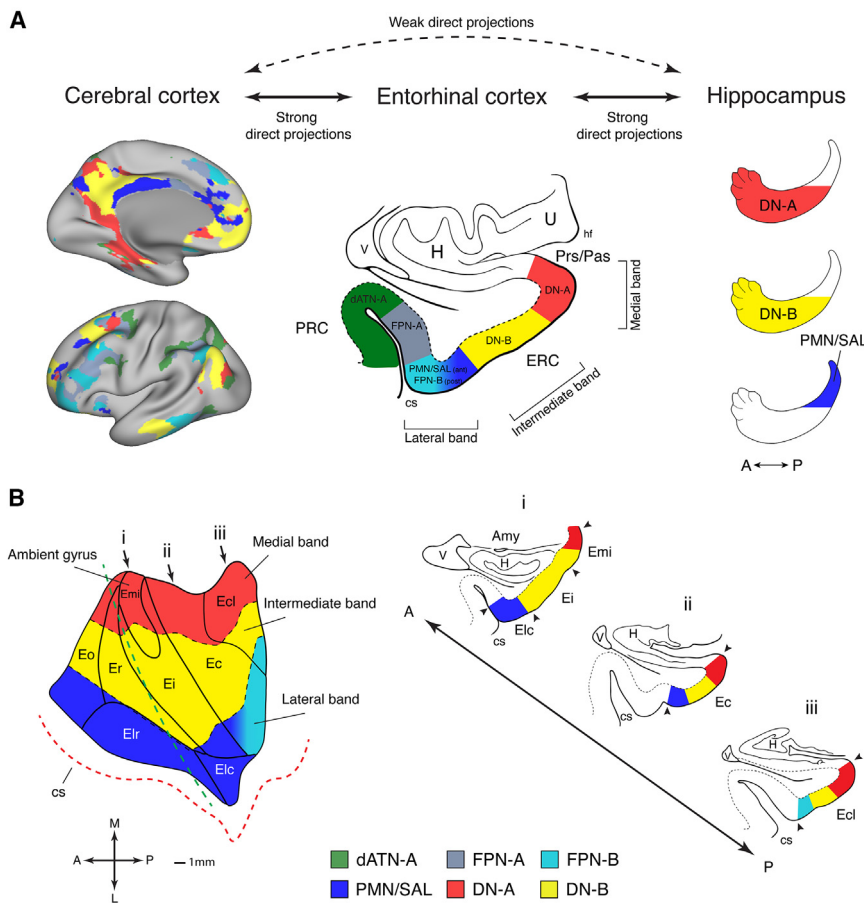


**Figure 5. Cortical networks of the hippocampal-entorhinal system**

(A) A summary illustration showing the cortical networks associated with the human medial temporal lobe. The cortical network DN-A is associated with the most medial part of the entorhinal cortex (closest to the hippocampus; medial band) and with the anterior part of the hippocampus (right to the coronal slice; red). Previously, we found that the cortical network DN-A is associated as well with the parahippocampal cortex (area TH, not shown; see Reznik et al.<sup>37</sup> for details). The cortical network DN-B is associated with the intermediate part of the entorhinal cortex (yellow; intermediate band) and with the anterior part of the hippocampus. The cortical networks PMN/SAL and FPN-B are associated with the most lateral parts of the entorhinal cortex (closest to the collateral sulcus; blue and cyan, respectively; lateral band); PMN/SAL is also associated with the posterior part of the hippocampus. Note that even though both PMN/SAL and FPN-B are displayed together on the same coronal slice, the cortical network PMN/SAL is associated with the anterior part of the lateral band and the cortical network FPN-B is associated with the posterior part of the lateral band. For completeness, we plotted the cortical networks we found to be associated with the perirhinal cortex—dATN-A<sup>37</sup> and FPN-A. The strength of direct anatomical projections (weak projections and strong projections), based on monkey tracing data, indicates cortical projections that originate from only a few or from more areas and/or projections that are less or more dense, respectively. See also Figure S5.

(B) *Left*: Group-level projection of the four cortical networks that we found to be associated with

the human entorhinal cortex to a template two-dimensional map of the human entorhinal cortex with cytoarchitecturally defined subfields (marked by solid black lines; adapted from Insausti et al.<sup>57</sup>). Note the clear arrangement of the cortical networks into three bands (marked by dashed black lines) that run almost in parallel to the collateral sulcus (red dashed line). It is important to mention that this map should be treated as an approximation because no cytoarchitectonic data were available and because we tested only four participants. Furthermore, we assigned the potential pre/parasubiculum to the medial band of the entorhinal cortex. Therefore, the medial band can be thinner than depicted when a more precise entorhinal-pre/parasubiculum boundary is considered. Finally, data anterior to the dashed green line were approximated due to reduced data quality in the most anterior parts of the entorhinal cortex. Despite these limitations, it is clear that the entorhinal bands traverse the cytoarchitectonic boundaries of entorhinal subfields. *Right*: Three coronal slices through the anterior-posterior axis of the entorhinal cortex (marked with i, ii, and iii on top of the two-dimensional map) displaying the band-like organization of the human entorhinal cortex. The coronal slices of the MTL were reproduced and adapted based on line drawings presented in Insausti et al.<sup>57</sup> Amy, amygdala; CS, collateral sulcus; ERC, entorhinal cortex; H, hippocampus; hf, hippocampal fissure; PRC, perirhinal cortex; Prs/Pas, pre/parasubiculum; U, uncus; V, temporal horn of the lateral ventricle. Entorhinal cortex subfields: Ec, entorhinal caudal; Ecl, entorhinal caudolateral; Ei, entorhinal intermediate; Elc, entorhinal lateral caudal; Elr, entorhinal lateral rostral; Emi, entorhinal medial intermediate; Eo, entorhinal olfactory; Er, entorhinal rostral. Directions: A, anterior; L, lateral; M, medial; P, posterior.

subfield.<sup>50,57</sup> Therefore, the association of the cortical network DN-A with the ambient gyrus supports the association of DN-A with both the most medial part of the entorhinal cortex and the pre/parasubiculum rather than with only the pre/parasubiculum. It is also possible that the association of the cortical network DN-A with the entorhinal cortex is more prevalent in the anterior entorhinal cortex than in the posterior entorhinal cortex, thus making the medial band of the entorhinal cortex potentially somewhat narrower in its posterior part.

We found that the cortical networks DN-A and DN-B are associated with the entire anterior-posterior axis of the entorhinal cortex (albeit in different positions on the medial-lateral axis). However, the cortical networks PMN/SAL and FPN-B are associated with the anterior and posterior parts of the lateral band of the entorhinal cortex, respectively. This finding is remarkably

consistent with animal anatomy showing that the most divergent connections with the broader neocortex exist between the anterior and posterior parts of the entorhinal lateral band, while the connections of the medial and intermediate bands of the entorhinal cortex are more homogeneous along the anterior-posterior axis<sup>13,60</sup> (Figure 5). Taken together, our results demonstrate that the human entorhinal cortex is associated with widely distributed cortical areas spanning the posteromedial cortex, parietal cortex, anterior cingulate cortex, the lateral surface of the temporal lobe, and medial and lateral prefrontal cortex (Figure 5A).

#### Distributed cortical processing associated with the hippocampus

Our findings indicating distinct cortical connectivity associated with the hippocampal longitudinal axis are consistent with



previous studies showing that the anterior hippocampus is predominantly associated with the cortical network DN-A, and the posterior hippocampus is predominantly associated with the cortical network PMN/SAL.<sup>40,41</sup> We add to these previous observations by showing that the anterior hippocampus is associated with the cortical network DN-B as well. Therefore, highly similar to the entorhinal cortex, we find that the human hippocampus is associated with the posteromedial cortex, parietal cortex, anterior cingulate cortex, anterior parts of the lateral surface of the temporal lobe, and ventromedial and lateral prefrontal cortex (Figure 5A). This may not be surprising in view of tract tracing studies indicating that most of the cortical input to the hippocampus originates in the entorhinal cortex. In fact, entorhinal cortex is the only cortical region providing input to the dentate gyrus, and direct cortical input to the hippocampus is minimal and mostly targets the border between CA1 and subiculum.<sup>5,61</sup>

Due to the limitations of fMRI connectivity methods, we could not differentiate between direct hippocampal-cortical connections and cortical connections that are mediated by the entorhinal cortex. Irrespective of this limitation, our findings are consistent with animal data pointing to a spatial connectivity gradient where the parts of the entorhinal cortex that are closer to the rhinal sulcus (collateral sulcus in humans) are associated with posterior hippocampus, and the parts of the entorhinal cortex that are closer to the hippocampus are associated with anterior hippocampus.<sup>6–9</sup> We found that the medial band of the entorhinal cortex, located closest to the hippocampus, is associated with the anterior hippocampus, and both are associated with the cortical network DN-A. On the other hand, the lateral band of the entorhinal cortex, located closest to the collateral sulcus, is associated with the posterior hippocampus, and both are associated with the cortical network PMN/SAL. Although our results show that the cortical network DN-B is associated with the entorhinal intermediate band, we did not observe the expected association of DN-B with the intermediate hippocampus<sup>52</sup> but found it to be associated with the anterior hippocampus instead. While we cannot rule out the possibility that both networks target similar regions within the human hippocampus, it is important to consider limitations of fMRI, such as geometrical distortions and spatial smoothing, in addressing this potential fine-grain anatomical dissociation.

### Convergence of distributed cortical processing in the entorhinal cortex

Our analysis, showing that the hippocampus and entorhinal cortex are characterized by a higher position on the unimodal-transmodal processing axis compared with other MTL subregions, suggests that the hippocampal-entorhinal system is the main convergence point of distributed cortical processing in the human memory system.<sup>62</sup> This finding is consistent with animal anatomy, which has shown that the entorhinal cortex is connected with the entire cortical mantle in the rodent<sup>53</sup> and with the notion that the convergence of a hierarchical organization of parallel processing streams culminates at the level of the hippocampal-entorhinal system.<sup>2</sup> Interestingly, connections of the parahippocampal cortex, perirhinal cortex, and entorhinal cortex likely changed in humans to prioritize connectivity with transmodal cortical areas at the expense of connections with unimodal cortical areas,<sup>63</sup> suggesting a greater functional role of

converging cortical processing in the entire hippocampal system. However, entorhinal cortex preserved its unique position as a cortical convergence hub compared with the parahippocampal cortex and the perirhinal cortex.

Moreover, examining the principal gradient values for each separate network associated with subregions of the MTL paints an intriguing picture. Although the apex of the principal gradient is typically discussed in the context of the canonical default network,<sup>55,64,65</sup> another cortical network that is positioned at the apex of the principal gradient is a subdivision of the canonical frontoparietal control network—FPN-B (Figure S5; see also Figure S4 in Margulies et al.<sup>55</sup>). Our results suggest that the two cortical networks positioned at the apex of the unimodal-transmodal processing axis, DN-B and FPN-B, are associated exclusively with the entorhinal cortex (and not with other MTL subregions), further supporting the role of the entorhinal cortex as one of the main convergence areas of cortical hierarchy in the human brain.

Finally, as can be seen in Figure 2, the spatial order of the cortical networks associated with the human MTL is not random. We observed a clear medial-to-lateral gradient in cortical network representations in the entorhinal cortex. When we also considered the cortical networks associated with the perirhinal cortex—FPN-A and dATN-A<sup>37</sup>—we observed that the order of the cortical networks in the anterior MTL followed the macroscale order in which the cortical networks repeatedly appear throughout the cortical mantle—dorsal attention networks, frontoparietal networks, and default networks<sup>47,55</sup> (Figure S5). This preliminary observation suggests that the hierarchy of information processing in anterior parts of human MTL follows a topographical rule that mirrors the macroscale structure of high-order cortical processing.

### Relations to prior observations and functional implications

Functional and structural studies in rodents have provided strong support to the notion that the entorhinal cortex might best be considered to comprise two subdivisions, generally referred to as lateral and medial entorhinal cortex.<sup>66</sup> In rats, these subdivisions can be easily differentiated using cytoarchitectonic analysis and patterns of anatomical connections with the hippocampus.<sup>67</sup> This notion, supported by findings in other species and partially in the macaque, has been influential in advancing the view that the hippocampal memory system is best considered a dual-stream system comprising parallel what (sensory) and where (spatial) processing networks. Although human and non-human primate entorhinal cortices can be cytoarchitectonically divided into multiple areas,<sup>57,68,69</sup> previous fMRI and diffusion tensor imaging studies found that the entorhinal cortex in humans can be subdivided into proposed homologs of rodent lateral and medial entorhinal cortices.<sup>25,28,70,71</sup> This notion was further supported by functional studies that showed that the proposed human homolog of the rodent lateral entorhinal cortex is best characterized by processing external information (e.g., temporal sequence and object-related information), and the proposed human homolog of the rodent medial entorhinal cortex is best characterized by spatial processing.<sup>16–22</sup>

Our current results showing a band-like organization of human entorhinal cortex can partly account for the previous

connectivity observations. We find that the anterior part of the entorhinal lateral band is more strongly connected with anterior cortical areas, such as the orbitofrontal cortex, whereas the entorhinal medial band is more strongly connected with posterior cortical areas, such as the retrosplenial cortex and parahippocampal cortex. These findings are consistent with the previously reported preferred connectivity of the putative human lateral and medial entorhinal cortex with the anterior and posterior memory systems, respectively.<sup>25–28</sup> In this study, using within-individual precision neuroimaging, we extend previous group-level observations and paint a more complex picture of cortical processing associated with the human entorhinal cortex.

Similar to our findings in humans, research into the anatomical and functional properties of the mammalian entorhinal cortex over the past 40 years indicates that the entire entorhinal cortex in rodents, non-human primates, and cats comprises three parallel band-like zones as well, running approximately in parallel to the rhinal sulcus.<sup>6–8,10</sup> Importantly, these bands are characterized by different connectivity with the neocortex, potentially indicating different, band-specific, functional specializations.<sup>13,60,72,73</sup> This principle of the entorhinal cortex as a matrix-like structure, organized along medial-lateral and anterior-posterior axes, can thus potentially represent a prototype of functional specialization within the human entorhinal cortex and the hippocampal-entorhinal system.

As we demonstrate, the entorhinal bands in humans are associated with distinct cortical networks. The most medial band is associated with the cortical network DN-A; a more laterally situated, intermediate band is associated with the cortical network DN-B; and the most lateral band, delimited by the collateral sulcus, is associated with the cortical networks FPN-A and PMN/SAL. Cortical networks DN-A and DN-B were previously shown to be involved in internally oriented cognitive processing.<sup>42</sup> Association of the human entorhinal cortex and hippocampus with the cortical network DN-A suggests involvement of these regions in spatial navigation and episodic recall/construction, which is supported by numerous prior observations.<sup>38,74–79</sup> The cortical network DN-B was previously shown to be preferably involved in social inference.<sup>38,80–82</sup> The association of the cortical network DN-B with the entorhinal cortex and hippocampus suggests involvement of these regions in social functions. Recent reports indicating connectivity of the default network, and specifically of DN-B, with the amygdala,<sup>83,84</sup> potentially complement the social circuit within the anterior portions of MTL involving the entorhinal cortex, hippocampus, and amygdala.<sup>85–90</sup>

Two other cortical networks, PMN/SAL and FPN-B, have been implicated in externally oriented cognitive processing.<sup>42,43</sup> A recent fMRI study in humans demonstrated that the cortical network PMN/SAL is involved in detecting changes in the external environment (see Angeli et al.<sup>41</sup> for discussion). This finding is consistent with rodent data attributing processing of the external environment to the dorsal hippocampus<sup>15</sup> and the lateral parts (closer to the rhinal sulcus) of the lateral entorhinal cortex.<sup>2</sup> Association of the human entorhinal cortex with the cortical network FPN-B suggests involvement of the entorhinal cortex in working memory.<sup>42,91,92,93</sup>

Furthermore, cortical connections of the human hippocampal-entorhinal system play an important role in cognitive mapping,

abstract structure learning, and reinforcement learning.<sup>94–100</sup> Outside of the hippocampal-entorhinal system, these cognitive processes were shown to be associated with a broad set of distributed cortical regions, such as the prefrontal cortex, posterior cingulate, and inferior parietal lobule. Most of these cortical regions overlap with the canonical default network,<sup>80</sup> which was proposed to support the construction of internal mental models, potentially corresponding to the construction of cognitive maps facilitating flexible behavior in spatial and non-spatial domains.<sup>96,97</sup> Our findings indicate that both subdivisions of the canonical default network (DN-A and DN-B) are associated with the hippocampal-entorhinal system, thus potentially supporting the formation of internal cognitive models by integrating spatial (DN-A) and non-spatial (DN-B) information.

Our results suggest that the human hippocampal-entorhinal system is a main convergence region of at least four distributed cortical processing systems in the human brain. Inspired by the parcellation of the rodent entorhinal cortex into lateral and medial subdivisions, it is common to characterize the functional properties of the entorhinal cortex in a dichotomous way, such as egocentric vs. allocentric representations<sup>101</sup> or what vs. where streams.<sup>26,102</sup> Although we currently cannot propose a general functional scheme accounting for each of the bands and their potential functional differentiation along the cytoarchitectonically defined division along the anterior-posterior axis, we nevertheless suggest that describing the functional properties of the human entorhinal cortex in terms of internal vs. external processing might better capture its functional complexity.

### Limitations

It is important to consider a few limitations pertaining to our study. The first limitation is fMRI data quality in the entorhinal cortex. Although our data collection was specifically optimized to reduce dropout and distortions in the anterior parts of the MTL, signal quality in the lateral and anterior portions of the entorhinal cortex was still considerably lower compared with signal quality in the posterior medial parts of the entorhinal cortex. To reduce noise, all available data from each participant that were not used for network estimation were used for independent exploration. This limitation is especially pronounced given our small sample size because we examined effects that were consistently present in all our participants. Therefore, it is highly likely that additional organization principles of human MTL will be discovered when better quality data from more participants will be considered. For example, the cortical network FPN-B was the only cortical network we found to be associated with the entorhinal cortex, but not with the hippocampus. Because we are not aware of an entorhinal region that does not share direct connections with the hippocampus in animals, we assume that this lack of evidence can be potentially attributed to limitations of our tools and methods. An additional limitation of our study pertains to anatomical interpretability of fMRI connectivity methods. Although correlations in intrinsic brain activity patterns are powerful tools for noninvasively studying anatomical connectivity,<sup>23,24</sup> these methods remain a proxy for anatomical connectivity. Therefore, in this study, we could not differentiate neither between input and output cortical connections of the hippocampal-entorhinal system nor between direct hippocampal-cortical connections and hippocampal connections with the broader cortex mediated by the entorhinal cortex.

## Conclusions

Using precision 7T fMRI data optimized for high-quality signal in the MTL, we characterized distributed cortical networks associated with the human hippocampal-entorhinal system and proposed a biologically plausible anatomical framework associating the human entorhinal cortex with the hippocampal longitudinal axis. Furthermore, we demonstrated that similar to other species in the mammalian lineage, the human entorhinal cortex is partitioned into three band-like zones that follow its anterior-posterior axis cutting through the proposed human homologs of the lateral and medial entorhinal cortex. Our results suggest that a comprehensive appreciation of the functional complexity associated with the human entorhinal cortex can benefit from examining its organizational principles that go beyond the long-standing quest for characterizing the human homologs of rodent lateral and medial entorhinal cortex.

## RESOURCE AVAILABILITY

### Lead contact

Further information and requests for resources should be directed to and will be fulfilled by the lead contact, Daniel Reznik ([reznik@cbs.mpg.de](mailto:reznik@cbs.mpg.de) or [reznikda@gmail.com](mailto:reznikda@gmail.com)).

### Materials availability

This study did not generate new unique reagents.

### Data and code availability

- Data used in this study were previously published in Reznik et al.<sup>37</sup>
- This paper does not report original code.
- Any additional information required to reanalyze the data reported in this paper is available from the [lead contact](#) upon request.

## ACKNOWLEDGMENTS

The authors thank Rebekka Tenderra, Rana Amini, and David Berron for helpful discussions and comments. Robert Trampel helped with data acquisition and piloting. Victoria Shevchenko and Austin Benn assisted with the cortical embedding analysis. This work is supported by the Max Planck Society. C.F.D.'s research is further supported by the European Research Council (ERC-CoG GEOCOG 724836), the Kavli Foundation, the Jebson Foundation, Helse Midt-Norge, and the Research Council of Norway (223262/F50; 197467/F50).

## AUTHOR CONTRIBUTIONS

D.R. and C.F.D. designed the study. D.R. analyzed the data with input from C.F.D., M.P.W., and D.S.M. D.R. wrote the original draft. D.R., M.P.W., D.S.M., and C.F.D. edited and wrote the manuscript. C.F.D. secured funding.

## DECLARATION OF INTERESTS

The authors declare no competing interests.

## STAR★METHODS

Detailed methods are provided in the online version of this paper and include the following:

- [KEY RESOURCES TABLE](#)
- [EXPERIMENTAL MODEL AND STUDY PARTICIPANT DETAILS](#)
  - Human participants
- [METHOD DETAILS](#)
  - Network definition: Cortical surface
  - Entorhinal cortex and hippocampus masks: Volumetric data

- Functional connectivity analysis: Network associations in the MTL
- Individualized gradient analysis
- Two-dimensional entorhinal cortex maps
- [QUANTIFICATION AND STATISTICAL ANALYSIS](#)

## SUPPLEMENTAL INFORMATION

Supplemental information can be found online at <https://doi.org/10.1016/j.cub.2024.10.020>.

Received: June 14, 2024

Revised: October 4, 2024

Accepted: October 5, 2024

Published: November 1, 2024

## REFERENCES

1. Lavenex, P., and Amaral, D.G. (2000). Hippocampal-neocortical interaction: A hierarchy of associativity. *Hippocampus* 10, 420–430. [https://doi.org/10.1002/1098-1063\(2000\)10:4<420::AID-HIPO8>3.0.CO;2-5](https://doi.org/10.1002/1098-1063(2000)10:4<420::AID-HIPO8>3.0.CO;2-5).
2. Nilssen, E.S., Doan, T.P., Nigro, M.J., Ohara, S., and Witter, M.P. (2019). Neurons and networks in the entorhinal cortex: A reappraisal of the lateral and medial entorhinal subdivisions mediating parallel cortical pathways. *Hippocampus* 29, 1238–1254. <https://doi.org/10.1002/hipo.23145>.
3. Insausti, R., Amaral, D.G., and Cowan, W.M. (1987). The entorhinal cortex of the monkey: II. Cortical afferents. *J. Comp. Neurol.* 264, 356–395. <https://doi.org/10.1002/cne.902640306>.
4. Burwell, R.D., and Amaral, D.G. (1998). Cortical afferents of the perirhinal, postrhinal, and entorhinal cortices of the rat. *J. Comp. Neurol.* 398, 179–205. [https://doi.org/10.1002/\(SICI\)1096-9861\(19980824\)398:2<179::AID-CNE3>3.0.CO;2-Y](https://doi.org/10.1002/(SICI)1096-9861(19980824)398:2<179::AID-CNE3>3.0.CO;2-Y).
5. Rosene, D.L., and Van Hoesen, G.W. (1987). The Hippocampal Formation of the Primate Brain. A Review of Some Comparative Aspects of Cytoarchitecture and Connections. In *Cerebral Cortex* (Plenum Publishing Corporation), pp. 345–456.
6. Witter, M.P., and Amaral, D.G. (1991). Entorhinal cortex of the monkey: V. Projections to the dentate gyrus, hippocampus, and subicular complex. *J. Comp. Neurol.* 307, 437–459. <https://doi.org/10.1002/CNE.903070308>.
7. Witter, M.P., and Amaral, D.G. (2021). The entorhinal cortex of the monkey: VI. Organization of projections from the hippocampus, subiculum, parasubiculum, and parasubiculum. *J. Comp. Neurol.* 529, 828–852. <https://doi.org/10.1002/cne.24983>.
8. van Groen, T., Miettinen, P., and Kadish, I. (2003). The entorhinal cortex of the mouse: Organization of the projection to the hippocampal formation. *Hippocampus* 13, 133–149. <https://doi.org/10.1002/HIPO.10037>.
9. Dolorfo, C.L., and Amaral, D.G. (1998). Entorhinal cortex of the rat: organization of intrinsic connections. *J. Comp. Neurol.* 398, 49–82. [https://doi.org/10.1002/\(SICI\)1096-9861\(19980817\)398:1<49::AID-CNE4>3.0.CO;2-9](https://doi.org/10.1002/(SICI)1096-9861(19980817)398:1<49::AID-CNE4>3.0.CO;2-9).
10. Witter, M.P., and Groenewegen, H.J. (1984). Laminar origin and septo-temporal distribution of entorhinal and perirhinal projections to the hippocampus in the cat. *J. Comp. Neurol.* 224, 371–385. <https://doi.org/10.1002/CNE.902240305>.
11. Jacobsen, B., Kleven, H., Gatome, W., Las, L., Ulanovsky, N., and Witter, M.P. (2023). Organization of projections from the entorhinal cortex to the hippocampal formation of the Egyptian fruit bat *Rousettus aegyptiacus*. *Hippocampus* 33, 889–905. <https://doi.org/10.1002/HIPO.23517>.
12. Insausti, R., and Amaral, D.G. (2008). Entorhinal cortex of the monkey: IV. Topographical and laminar organization of cortical afferents. *J. Comp. Neurol.* 509, 608–641. <https://doi.org/10.1002/cne.21753>.
13. Burwell, R.D. (2000). The parahippocampal region: corticocortical connectivity. *Annals of the New York Academy of Sciences* 911, 25–42. <https://doi.org/10.1111/j.1749-6632.2000.tb06717.x>.

14. Strange, B.A., Witter, M.P., Lein, E.S., and Moser, E.I. (2014). Functional organization of the hippocampal longitudinal axis. *Nat. Rev. Neurosci.* *15*, 655–669. <https://doi.org/10.1038/nrn3785>.
15. Moser, M.B., and Moser, E.I. (1998). Functional differentiation in the hippocampus. *Hippocampus* *8*, 608–619. [https://doi.org/10.1002/\(SICI\)1098-1063\(1998\)8:6<608::AID-HIPO3>3.0.CO;2-7](https://doi.org/10.1002/(SICI)1098-1063(1998)8:6<608::AID-HIPO3>3.0.CO;2-7).
16. Reagh, Z.M., and Yassa, M.A. (2014). Object and spatial mnemonic interference differentially engage lateral and medial entorhinal cortex in humans. *Proc. Natl. Acad. Sci. USA* *111*, E4264–E4273. <https://doi.org/10.1073/pnas.1411250111>.
17. Schultz, H., Sommer, T., and Peters, J. (2012). Direct evidence for domain-sensitive functional subregions in human entorhinal cortex. *J. Neurosci.* *32*, 4716–4723. <https://doi.org/10.1523/JNEUROSCI.5126-11.2012>.
18. Yeung, L.-K., Olsen, R.K., Hong, B., Mihajlovic, V., D'Angelo, M.C., Kacollja, A., Ryan, J.D., and Barense, M.D. (2019). Object-in-place memory predicted by anterolateral entorhinal cortex and parahippocampal cortex volume in older adults. *J. Cogn. Neurosci.* *31*, 711–729. [https://doi.org/10.1162/jocn\\_a\\_01385](https://doi.org/10.1162/jocn_a_01385).
19. Yeung, L.-K., Olsen, R.K., Bild-Enkin, H.E.P., D'Angelo, M.C., Kacollja, A., McQuiggan, D.A., Keshabyan, A., Ryan, J.D., and Barense, M.D. (2017). Anterolateral entorhinal cortex volume predicted by altered intra-atem configural processing. *J. Neurosci.* *37*, 5527–5538. <https://doi.org/10.1523/JNEUROSCI.3664-16.2017>.
20. Ferko, K.M., Blumenthal, A., Martin, C.B., Proklova, D., Minos, A.N., Saksida, L.M., Bussey, T.J., Khan, A.R., and Köhler, S. (2022). Activity in perirhinal and entorhinal cortex predicts perceived visual similarities among category exemplars with highest precision. *eLife* *11*, <https://doi.org/10.7554/eLife.66884>.
21. Bellmund, J.L., Deuker, L., and Doeller, C.F. (2019). Mapping sequence structure in the human lateral entorhinal cortex. *eLife* *8*, <https://doi.org/10.7554/eLife.45333>.
22. Montchal, M.E., Reagh, Z.M., and Yassa, M.A. (2019). Precise temporal memories are supported by the lateral entorhinal cortex in humans. *Nat. Neurosci.* *22*, 284–288. <https://doi.org/10.1038/s41593-018-0303-1>.
23. Vincent, J.L., Patel, G.H., Fox, M.D., Snyder, A.Z., Baker, J.T., Van Essen, D.C., Zempel, J.M., Snyder, L.H., Corbetta, M., and Raichle, M.E. (2007). Intrinsic functional architecture in the anaesthetized monkey brain. *Nature* *447*, 83–86. <https://doi.org/10.1038/nature05758>.
24. Liu, C., Yen, C.C.C., Szczupak, D., Ye, F.Q., Leopold, D.A., and Silva, A.C. (2019). Anatomical and functional investigation of the marmoset default mode network. *Nat. Commun.* *10*, 1975. <https://doi.org/10.1038/s41467-019-09813-7>.
25. Navarro Schröder, T., Haak, K.V., Zaragoza Jimenez, N.I., Beckmann, C.F., and Doeller, C.F. (2015). Functional topography of the human entorhinal cortex. *eLife* *4*, e06738. <https://doi.org/10.7554/eLife.06738>.
26. Ranganath, C., and Ritchey, M. (2012). Two cortical systems for memory-guided behaviour. *Nat. Rev. Neurosci.* *13*, 713–726. <https://doi.org/10.1038/nrn3338>.
27. Ritchey, M., Libby, L.A., and Ranganath, C. (2015). Cortico-hippocampal systems involved in memory and cognition: The PMAT framework. *Prog. Brain Res.* *219*, 45–64. <https://doi.org/10.1016/bs.pbr.2015.04.001>.
28. Maass, A., Berron, D., Libby, L.A., Ranganath, C., and Düzel, E. (2015). Functional subregions of the human entorhinal cortex. *eLife* *4*, e06426. <https://doi.org/10.7554/eLife.06426>.
29. Dalton, M.A., McCormick, C., and Maguire, E.A. (2019). Differences in functional connectivity along the anterior-posterior axis of human hippocampal subfields. *Neuroimage* *192*, 38–51. <https://doi.org/10.1016/j.neuroimage.2019.02.066>.
30. Dalton, M.A., D'Souza, A., Lv, J., and Calamante, F. (2022). New insights into anatomical connectivity along the anterior-posterior axis of the human hippocampus using in vivo quantitative fibre tracking. *eLife* *11*, <https://doi.org/10.7554/eLife.76143>.
31. Jung, M.W., Wiener, S.I., and McNaughton, B.L. (1994). Comparison of Spatial Firing Characteristics of Units in Dorsal and Ventral Hippocampus of the Rat. *J. Neurosci.* *14*, 7347–7356. <https://doi.org/10.1523/JNEUROSCI.14-12-07347.1994>.
32. Woollett, K., and Maguire, E.A. (2005). Report Acquiring “the Knowledge” of London’s Layout Drives Structural Brain Changes. *Curr. Biol.* *21*, 2109–2114. <https://doi.org/10.1016/j.cub.2011.11.018>.
33. Addis, D.R., Moscovitch, M., Crawley, A.P., and McAndrews, M.P. (2004). Recollective Qualities Modulate Hippocampal Activation During Autobiographical Memory Retrieval. *Hippocampus* *14*, 752–762. <https://doi.org/10.1002/hipo.10215>.
34. Hirshhorn, M., Grady, C., Rosenbaum, R.S., Winocur, G., and Moscovitch, M. (2012). Brain regions involved in the retrieval of spatial and episodic details associated with a familiar environment: An fMRI study. *Neuropsychologia* *50*, 3094–3106. <https://doi.org/10.1016/j.neuropsychologia.2012.08.008>.
35. Poppenk, J., Evensmoen, H.R., Moscovitch, M., and Nadel, L. (2013). Long-axis specialization of the human hippocampus. *Trends Cogn. Sci.* *17*, 230–240. <https://doi.org/10.1016/j.tics.2013.03.005>.
36. Gordon, E.M., Laumann, T.O., Gilmore, A.W., Newbold, D.J., Greene, D.J., Berg, J.J., Ortega, M., Hoyt-Drazen, C., Grattton, C., Sun, H., et al. (2017). Precision Functional Mapping of Individual Human Brains. *Neuron* *95*, 791–807.e7. <https://doi.org/10.1016/j.neuron.2017.07.011>.
37. Reznik, D., Trampel, R., Weiskopf, N., Witter, M.P., and Doeller, C.F. (2023). Dissociating distinct cortical networks associated with subregions of the human medial temporal lobe using precision neuroimaging. *Neuron* *111*, 2756–2772.e7. <https://doi.org/10.1016/j.neuron.2023.05.029>.
38. DiNicola, L.M., Braga, R.M., and Buckner, R.L. (2020). Parallel distributed networks dissociate episodic and social functions within the individual. *J. Neurophysiol.* *123*, 1144–1179. <https://doi.org/10.1152/jn.00529.2019>.
39. Braga, R.M., and Buckner, R.L. (2017). Parallel Interdigitated Distributed Networks within the Individual Estimated by Intrinsic Functional Connectivity. *Neuron* *95*, 457–471.e5. <https://doi.org/10.1016/j.neuron.2017.06.038>.
40. Zheng, A., Montez, D.F., Marek, S., Gilmore, A.W., Newbold, D.J., Laumann, T.O., Kay, B.P., Seider, N.A., Van, A.N., Hampton, J.M., et al. (2021). Parallel hippocampal-parietal circuits for self- And goal-oriented processing. *Proc. Natl. Acad. Sci. USA* *118*, e2101743118. <https://doi.org/10.1073/PNAS.2101743118>.
41. Angeli, P.A., Dinicola, L.M., Saadon-Grosman, N., Eldaief, M.C., and Buckner, R.L. (2023). Specialization of the Human Hippocampal Long Axis Revisited. Preprint at bioRxiv. <https://doi.org/10.1101/2023.12.19.572264>.
42. Du, J., Dinicola, L.M., Angeli, P.A., Saadon-Grosman, N., Sun, W., Kaiser, S., Ladopoulou, J., Xue, A., Yeo, B.T.T., Eldaief, M.C., et al. (2024). Organization of the Human Cerebral Cortex Estimated Within Individuals: Networks, Global Topography, and Function. *J. Neurophysiol.* *131*, 1014–1082. <https://doi.org/10.1152/jn.00308.2023>.
43. Seeley, W.W., Menon, V., Schatzberg, A.F., Keller, J., Glover, G.H., Kenna, H., Reiss, A.L., and Greicius, M.D. (2007). Dissociable Intrinsic Connectivity Networks for Salience Processing and Executive Control. *J. Neurosci.* *27*, 2349–2356. <https://doi.org/10.1523/JNEUROSCI.5587-06.2007>.
44. Gilmore, A.W., Nelson, S.M., and McDermott, K.B. (2015). A parietal memory network revealed by multiple MRI methods. *Trends Cogn. Sci.* *19*, 534–543. <https://doi.org/10.1016/j.tics.2015.07.004>.
45. Kwon, Y., Salvo, J.J., Anderson, N., Holubecki, A.M., Lakshman, M., Yoo, K., Kay, K., Grattton, C., and Braga, R.M. (2023). Situating the parietal memory network in the context of multiple parallel distributed networks using high-resolution functional connectivity. Preprint at bioRxiv. <https://doi.org/10.1101/2023.08.16.553585>.
46. Vincent, J.L., Kahn, I., Snyder, A.Z., Raichle, M.E., and Buckner, R.L. (2008). Evidence for a frontoparietal control system revealed by intrinsic



- functional connectivity. *J. Neurophysiol.* 100, 3328–3342. <https://doi.org/10.1152/jn.90355.2008>.
47. Yeo, B.T.T., Krienen, F.M., Sepulcre, J., Sabuncu, M.R., Lashkari, D., Hollinshead, M., Roffman, J.L., Smoller, J.W., Zöllei, L., Polimeni, J.R., et al. (2011). The organization of the human cerebral cortex estimated by intrinsic functional connectivity. *J. Neurophysiol.* 106, 1125–1165. <https://doi.org/10.1152/jn.00338.2011>.
  48. Kibro-Flatmoen, A., and Witter, M.P. (2019). Neuronal chemo-architecture of the entorhinal cortex: A comparative review. *Eur. J. Neurosci.* 50, 3627–3662. <https://doi.org/10.1111/ejn.14511>.
  49. Canto, C.B., and Witter, M.P. (2012). Cellular Properties of Principal Neurons in the Rat Entorhinal Cortex. II. The Medial Entorhinal Cortex. *Hippocampus* 22, 1277–1299. <https://doi.org/10.1002/hipo.20993>.
  50. Insausti, R., Córcoles-Parada, M., Ubero, M.M., Rodado, A., Insausti, A.M., and Muñoz-López, M. (2019). Cytoarchitectonic Areas of the Gyrus ambiens in the Human Brain. *Front. Neuroanat.* 13, 21. <https://doi.org/10.3389/fnana.2019.00021>.
  51. Greene, D.J., Marek, S., Gordon, E.M., Siegel, J.S., Gratton, C., Laumann, T.O., Gilmore, A.W., Berg, J.J., Nguyen, A.L., Dierker, D., et al. (2020). Integrative and Network-Specific Connectivity of the Basal Ganglia and Thalamus Defined in Individuals. *Neuron* 105, 742–758.e6. <https://doi.org/10.1016/j.neuron.2019.11.012>.
  52. Bast, T., Wilson, I.A., Witter, M.P., and Morris, R.G.M. (2009). From Rapid Place Learning to Behavioral Performance: A Key Role for the Intermediate Hippocampus. *PLoS Biol.* 7, e1000089. <https://doi.org/10.1371/journal.pbio.1000089>.
  53. Bota, M., Sporns, O., and Swanson, L.W. (2015). Architecture of the cerebral cortical association connectome underlying cognition. *Proc. Natl. Acad. Sci. USA* 112, E2093–E2101. <https://doi.org/10.1073/pnas.1504394112>.
  54. Felleman, D.J., and Van Essen, D.C. (1991). Distributed hierarchical processing in the primate cerebral cortex. *Cereb. Cortex* 1, 1–47. <https://doi.org/10.1093/cercor/1.1.1-a>.
  55. Margulies, D.S., Ghosh, S.S., Goulas, A., Falkiewicz, M., Huntenburg, J.M., Langs, G., Bezgin, G., Eickhoff, S.B., Castellanos, F.X., Petrides, M., et al. (2016). Situating the default-mode network along a principal gradient of macroscale cortical organization. *Proc. Natl. Acad. Sci. USA* 113, 12574–12579. <https://doi.org/10.1073/pnas.1608282113>.
  56. Petersen, S.E., Seitzman, B.A., Nelson, S.M., Wig, G.S., and Gordon, E.M. (2024). Principles of cortical areas and their implications for neuroimaging. *Neuron* 112, 2837–2853. <https://doi.org/10.1016/J.NEURON.2024.05.008>.
  57. Insausti, R., Tuñón, T., Sobreviela, T., Insausti, A.M., and Gonzalo, L.M. (1995). The human entorhinal cortex: A cytoarchitectonic analysis. *J. Comp. Neurol.* 355, 171–198. <https://doi.org/10.1002/cne.903550203>.
  58. Braga, R.M., Van Dijk, K.R.A., Polimeni, J.R., Eldaief, M.C., and Buckner, R.L. (2019). Parallel distributed networks resolved at high resolution reveal close juxtaposition of distinct regions. *J. Neurophysiol.* 121, 1513–1534. <https://doi.org/10.1152/jn.00808.2018>.
  59. Boccara, C.N., Sargolini, F., Thoresen, V.H., Solstad, T., Witter, M.P., Moser, E.I., and Moser, M.-B. (2010). Grid cells in pre- and parasubiculum. *Nat. Neurosci.* 13, 987–994. <https://doi.org/10.1038/nrn.2602>.
  60. Insausti, R., Herrero, M.T., and Witter, M.P. (1997). Entorhinal cortex of the rat: Cytoarchitectonic subdivisions and the origin and distribution of cortical efferents. *Hippocampus* 7, 146–183. [https://doi.org/10.1002/\(SICI\)1098-1063\(1997\)7:2<146::AID-HIPO4>3.0.CO;2-L](https://doi.org/10.1002/(SICI)1098-1063(1997)7:2<146::AID-HIPO4>3.0.CO;2-L).
  61. Morris, R.E., Pandya, D.N., and Petrides, M. (1999). Fiber System Linking the Mid-Dorsolateral Frontal Cortex With the Retrosplenial/Presubicular Region in the Rhesus Monkey. *J. Comp. Neurol.* 407, 183–192. [https://doi.org/10.1002/\(SICI\)1096-9861\(19990503\)407:2<183::AID-CNE3>3.0.CO;2-N](https://doi.org/10.1002/(SICI)1096-9861(19990503)407:2<183::AID-CNE3>3.0.CO;2-N).
  62. Backus, A.R., Bosch, S.E., Ekman, M., Grabovetsky, A.V., and Doeller, C.F. (2016). Mnemonic convergence in the human hippocampus. *Nat. Commun.* 7, 11991. <https://doi.org/10.1038/ncomms11991>.
  63. Reznik, D., Majka, P., Rosa, M.G., Witter, M.P., and Doeller, C.F. (2024). Phylogeny of neocortical-hippocampal projections provides insight in the nature of human memory. *eLife* 13, <https://doi.org/10.7554/ELIFE.99203.1>.
  64. Buckner, R.L., and Margulies, D.S. (2019). Macroscale cortical organization and a default-like apex transmodal network in the marmoset monkey. *Nat. Commun.* 10, 1976. <https://doi.org/10.1038/s41467-019-09812-8>.
  65. Smallwood, J., Bernhardt, B.C., Leech, R., Bzdok, D., Jefferies, E., and Margulies, D.S. (2021). The default mode network in cognition: a topographical perspective. *Nat. Rev. Neurosci.* 22, 503–513. <https://doi.org/10.1038/s41583-021-00474-4>.
  66. Kerr, K.M., Agster, K.L., Furtak, S.C., and Burwell, R.D. (2007). Functional neuroanatomy of the parahippocampal region: The lateral and medial entorhinal areas. *Hippocampus* 17, 697–708. <https://doi.org/10.1002/hipo.20315>.
  67. Witter, M.P. (2007). The perforant path: projections from the entorhinal cortex to the dentate gyrus. *Prog. Brain Res.* 163, 43–61. [https://doi.org/10.1016/S0079-6123\(07\)63003-9](https://doi.org/10.1016/S0079-6123(07)63003-9).
  68. Insausti, R. (1993). Comparative anatomy of the entorhinal cortex and hippocampus in mammals. *Hippocampus* 3, 19–26. <https://doi.org/10.1002/hipo.1993.4500030705>.
  69. Amaral, D.G., Insausti, R., and Cowan, W.M. (1987). The entorhinal cortex of the monkey: I. Cytoarchitectonic organization. *J. Comp. Neurol.* 264, 326–355. <https://doi.org/10.1002/CNE.902640305>.
  70. Syversen, I.F., Witter, M.P., Kibro-Flatmoen, A., Goa, P.E., Navarro Schröder, T., and Doeller, C.F. (2021). Structural connectivity-based segmentation of the human entorhinal cortex. *Neuroimage* 245, 118723. <https://doi.org/10.1016/J.NEUROIMAGE.2021.118723>.
  71. Syversen, I.F., Reznik, D., Menno, J., Witter, P., Kibro-Flatmoen, A., Tobias, J., Schröder, N., Christian, J., and Doeller, F. (2024). A combined DTI-fMRI approach for optimizing the delineation of posteromedial versus anterolateral entorhinal cortex. *Hippocampus*, 1–14. <https://doi.org/10.1002/HIPO.23639>.
  72. Witter, M.P., Groenewegen, H.J., Lopes da Silva, F.H., and Lohman, A.H.M. (1989). Functional organization of the extrinsic and intrinsic circuitry of the parahippocampal region. *Prog. Neurobiol.* 33, 161–253. [https://doi.org/10.1016/0301-0082\(89\)90009-9](https://doi.org/10.1016/0301-0082(89)90009-9).
  73. Steffenach, H.-A., Witter, M., Moser, M.-B., and Moser, E.I. (2005). Spatial Memory in the Rat Requires the Dorsolateral Band of the Entorhinal Cortex. *Neuron* 45, 301–313. <https://doi.org/10.1016/j.neuron.2004.12.044>.
  74. Burgess, N., Maguire, E.A., and O'Keefe, J. (2002). The Human Hippocampus and Spatial and Episodic Memory. *Neuron* 35, 625–641. [https://doi.org/10.1016/S0896-6273\(02\)00830-9](https://doi.org/10.1016/S0896-6273(02)00830-9).
  75. Hassabis, D., and Maguire, E.A. (2007). Deconstructing episodic memory with construction. *Trends Cogn. Sci.* 11, 299–306. <https://doi.org/10.1016/j.tics.2007.05.001>.
  76. Zeidman, P., and Maguire, E.A. (2016). Anterior hippocampus: The anatomy of perception, imagination and episodic memory. *Nat. Rev. Neurosci.* 17, 173–182. <https://doi.org/10.1038/nrn.2015.24>.
  77. Doeller, C.F., Barry, C., and Burgess, N. (2010). Evidence for grid cells in a human memory network. *Nature* 463, 657–661. <https://doi.org/10.1038/nature08704>.
  78. Leonard, B.W., Amaral, D.G., Squire, L.F., Zola-Morgan, S., and S.. (1995). Transient Memory Impairment in Monkeys with Bilateral Lesions of the Entorhinal Cortex. *J. Neurosci.* 15, 5637–5659. <https://doi.org/10.1523/JNEUROSCI.15-08-05637.1995>.
  79. Buckmaster, C.A., Eichenbaum, H., Amaral, D.G., Suzuki, W.A., and Rapp, P.R. (2004). Entorhinal Cortex Lesions Disrupt the Relational Organization of Memory in Monkeys. *J. Neurosci.* 24, 9811–9825. <https://doi.org/10.1523/JNEUROSCI.1532-04.2004>.

80. Buckner, R.L., and DiNicola, L.M. (2019). The brain's default network: updated anatomy, physiology and evolving insights. *Nat. Rev. Neurosci.* 20, 593–608. <https://doi.org/10.1038/s41583-019-0212-7>.
81. Andrews-Hanna, J.R., Saxe, R., and Yarkoni, T. (2014). Contributions of episodic retrieval and mentalizing to autobiographical thought: Evidence from functional neuroimaging, resting-state connectivity, and fMRI meta-analyses. *Neuroimage* 91, 324–335. <https://doi.org/10.1016/j.neuroimage.2014.01.032>.
82. Saxe, R., and Kanwisher, N. (2013). People Thinking about Thinking People: The Role of the Temporo-parietal Junction in “Theory of Mind.” *Social Neuroscience*, 171–182.
83. Sylvester, C.M., Yu, Q., Srivastava, A.B., Marek, S., Zheng, A., Alexopoulos, D., Smyser, C.D., Shimony, J.S., Ortega, M., Dierker, D.L., et al. (2020). Individual-specific functional connectivity of the amygdala: A substrate for precision psychiatry. *Proc. Natl. Acad. Sci. USA* 117, 3808–3818. <https://doi.org/10.1073/pnas.1910842117>.
84. Edmonds, D., Salvo, J.J., Anderson, N., Lakshman, M., Yang, Q., Kay, K., Zelano, C., and Braga, R.M. (2024). Social cognitive regions of human association cortex are selectively connected to the amygdala. Preprint at bioRxiv. <https://doi.org/10.1101/2023.12.06.570477>.
85. Tavares, R.M., Mendelsohn, A., Grossman, Y., Williams, C.H., Shapiro, M., Trope, Y., and Schiller, D. (2015). A Map for Social Navigation in the Human Brain. *Neuron* 87, 231–243. <https://doi.org/10.1016/j.neuron.2015.06.011>.
86. Adolphs, R. (2010). What does the amygdala contribute to social cognition? *Ann. N. Y. Acad. Sci.* 1191, 42–61. <https://doi.org/10.1111/j.1749-6632.2010.05445.x>.
87. Omer, D.B., Maimon, S.R., Las, L., and Ulanovsky, N. (2018). Social place-cells in the bat hippocampus. *Science* 359, 218–224. <https://doi.org/10.1126/science.aao3474>.
88. Danjo, T., Toyozumi, T., and Fujisawa, S. (2018). Spatial representations of self and other in the hippocampus. *Science* 359, 213–218. <https://doi.org/10.1126/science.aao3898>.
89. Banker, S.M., Gu, X., Schiller, D., and Foss-Feig, J.H. (2021). Hippocampal contributions to social and cognitive deficits in autism spectrum disorder. *Trends Neurosci.* 44, 793–807. <https://doi.org/10.1016/j.tins.2021.08.005>.
90. Petrucci, A., Alvarez, P., and Eichenbaum, H. (2005). Neural correlates of social odor recognition and the representation of individual distinctive social odors within entorhinal cortex and ventral subiculum. *Neuroscience* 130, 259–274. <https://doi.org/10.1016/j.neuroscience.2004.09.001>.
91. Mazoyer, B., Zago, L., Mellet, E., Bricogne, S., Etard, O., Houdé, O., Crivello, F., Joliot, M., Petit, L., and Tzourio-Mazoyer, N. (2001). Cortical networks for working memory and executive functions sustain the conscious resting state in man. *Brain Res. Bull.* 54, 287–298. [https://doi.org/10.1016/s0361-9230\(00\)00437-8](https://doi.org/10.1016/s0361-9230(00)00437-8).
92. Saylik, R., Williams, A.L., Murphy, R.A., and Szameitat, A.J. (2022). Characterising the unity and diversity of executive functions in a within-subject fMRI study. *Sci. Rep.* 12, 8182. <https://doi.org/10.1038/s41598-022-11433-z>.
93. Newmark, R.E., Schon, K., Ross, R.S., and Stern, C.E. (2013). Contributions of the hippocampal subfields and entorhinal cortex to disambiguation during working memory. *Hippocampus* 23, 467–475. <https://doi.org/10.1002/hipo.22106>.
94. Tolman, E.C. (1948). Cognitive maps in rats and men. *Psychol. Rev.* 55, 189–208. <https://doi.org/10.1037/h0061626>.
95. Constantinescu, A.O., O'Reilly, J.X., and Behrens, T.E.J. (2016). Organizing conceptual knowledge in humans with a gridlike code. *Science* 352, 1464–1468. <https://doi.org/10.1126/science.aaf0941>.
96. Behrens, T.E.J., Muller, T.H., Whittington, J.C.R., Mark, S., Baram, A.B., Stachenfeld, K.L., and Kurth-Nelson, Z. (2018). What Is a Cognitive Map? Organizing Knowledge for Flexible Behavior. *Neuron* 100, 490–509. <https://doi.org/10.1016/j.neuron.2018.10.002>.
97. Bellmund, J.L.S., Gärdenfors, P., Moser, E.I., and Doeller, C.F. (2018). Navigating cognition: Spatial codes for human thinking. *Science* 362, eaat6766. <https://doi.org/10.1126/science.aat6766>.
98. Bottini, R., and Doeller, C.F. (2020). Knowledge Across Reference Frames: Cognitive Maps and Image Spaces. *Trends Cogn. Sci.* 24, 606–619. <https://doi.org/10.1016/j.tics.2020.05.008>.
99. Theves, S., Fernandez, G., and Doeller, C.F. (2019). The Hippocampus Encodes Distances in Multidimensional Feature Space. *Curr. Biol.* 29, 1226–1231.e3. <https://doi.org/10.1016/j.cub.2019.02.035>.
100. Garvert, M.M., Saanum, T., Schulz, E., Schuck, N.W., and Doeller, C.F. (2023). Hippocampal spatio-predictive cognitive maps adaptively guide reward generalization. *Nat. Neurosci.* 26, 615–626. <https://doi.org/10.1038/s41593-023-01283-x>.
101. Wang, C., Chen, X., and Knierim, J.J. (2020). Egocentric and allocentric representations of space in the rodent brain. *Curr. Opin. Neurobiol.* 60, 12–20. <https://doi.org/10.1016/j.conb.2019.11.005>.
102. Eichenbaum, H., Yonelinas, A.P., and Ranganath, C. (2007). The medial temporal lobe and recognition memory. *Annu. Rev. Neurosci.* 30, 123–152. <https://doi.org/10.1146/annurev.neuro.30.051606.094328>.
103. Marcus, D.S., Harwell, J., Olsen, T., Hodge, M., Glasser, M.F., Prior, F., Jenkinson, M., Laumann, T., Curtiss, S.W., and Van Essen, D.C. (2011). Informatics and data mining tools and strategies for the human connectome project. *Front. Neuroinform.* 5, 4. <https://doi.org/10.3389/fninf.2011.00004>.
104. Fischl, B. (2012). FreeSurfer. *Neuroimage* 62, 774–781. <https://doi.org/10.1016/j.neuroimage.2012.01.021>.
105. Kong, R., Li, J., Orban, C., Sabuncu, M.R., Liu, H., Schaefer, A., Sun, N., Zuo, X.-N., Holmes, A.J., Eickhoff, S.B., et al. (2019). Spatial Topography of Individual-Specific Cortical Networks Predicts Human Cognition, Personality, and Emotion. *Cereb. Cortex* 29, 2533–2551. <https://doi.org/10.1093/cercor/bhy123>.
106. Laumann, T.O., Gordon, E.M., Adeyemo, B., Snyder, A.Z., Joo, S.J., Chen, M.Y., Gilmore, A.W., McDermott, K.B., Nelson, S.M., Dosenbach, N.U.F., et al. (2015). Functional System and Areal Organization of a Highly Sampled Individual Human Brain. *Neuron* 87, 657–670. <https://doi.org/10.1016/j.neuron.2015.06.037>.
107. Insausti, R., Insausti, A.M., Sobreviela, M.T., Salinas, A., and Martínez-Peñuela, J.M. (1998). Human medial temporal lobe in aging: Anatomical basis of memory preservation. *Microsc. Res. Tech.* 43, 8–15. [https://doi.org/10.1002/\(SICI\)1097-0029\(19981001\)43:1<8::AID-JEMT2>3.0.CO;2-4](https://doi.org/10.1002/(SICI)1097-0029(19981001)43:1<8::AID-JEMT2>3.0.CO;2-4).
108. Insausti, R., Juottonen, K., Soininen, H., Insausti, A.M., Partanen, K., Vainio, P., Laakso, M.P., and Pitkänen, A. (1998). MR volumetric analysis of the human entorhinal, perirhinal, and temporopolar cortices. *AJNR Am. J. Neurorad.* 19, 659–671.
109. Wuestefeld, A., Baumeister, H., Adams, J.N., de Flores, R., Hodgetts, C.J., Mazloum-Farzaghi, N., Olsen, R.K., Puliyadi, V., Tran, T.T., Bakker, A., et al. (2024). Comparison of histological delineations of medial temporal lobe cortices by four independent neuroanatomy laboratories. *Hippocampus* 34, 241–260. <https://doi.org/10.1002/hipo.23602>.

## STAR★METHODS

### KEY RESOURCES TABLE

REAGENT or RESOURCE	SOURCE	IDENTIFIER
Software and algorithms		
Connectome Workbench	Marcus et al. <sup>103</sup>	<a href="http://www.humanconnectome.org/software/connectome-workbench">http://www.humanconnectome.org/software/connectome-workbench</a>
FreeSurfer	Fischl <sup>104</sup>	<a href="https://surfer.nmr.mgh.harvard.edu/">https://surfer.nmr.mgh.harvard.edu/</a>
MATLAB	Mathworks	<a href="https://www.mathworks.com/">https://www.mathworks.com/</a>
MATLAB code for Connectome Workbench	–	<a href="https://github.com/Washington-University/cifti-matlab">https://github.com/Washington-University/cifti-matlab</a>
MATLAB code for MS-HBM	Kong et al. <sup>105</sup>	<a href="https://github.com/ThomasYeoLab/CBIG/tree/master">https://github.com/ThomasYeoLab/CBIG/tree/master</a>

### EXPERIMENTAL MODEL AND STUDY PARTICIPANT DETAILS

#### Human participants

In this study, we used our previously reported fMRI fixation task (resting-state) dataset specifically optimized for high signal quality in the MTL.<sup>37</sup> In short, four healthy human participants were scanned during four separate 7T MRI sessions comprising eight fixation tasks, each lasting seven minutes and 28 seconds. Functional data processing was optimized for within-subject analysis to preserve anatomical detail and reduce blurring across different scanning sessions (see Reznik et al.<sup>37</sup> and Braga et al.<sup>58</sup> for more details). Overall, about 240 min of whole-brain blood-oxygen-level-dependent (BOLD) data with isotropic spatial resolution of 1.5 mm were acquired for each participant. See Reznik et al.<sup>37</sup> for a detailed description of the data acquisition parameters, within-participant processing and quality control procedures.

### METHOD DETAILS

#### Network definition: Cortical surface

To prepare the data for cortical parcellation, processed volumetric data were resampled to the fsaverage6 standardized cortical surface mesh (40,962 vertices per hemisphere) and spatially smoothed using a 4 mm full width at half maximum (FWHM) kernel. To avoid bias, we dissociated the network estimation procedure and network-based exploration of the hippocampal-entorhinal system by constructing two separate datasets from all BOLD data available for each participant. In each participant, the network estimation dataset comprised eight fixation task runs, resulting in about one hour of BOLD data, which was shown to be sufficient for reliable network estimation within individuals.<sup>106</sup> For network estimation, we used multi-session hierarchical Bayesian modelling<sup>105</sup> (MS-HBM) to identify distributed cortical networks in each individual. Our previous seed-based investigation of the entorhinal cortex pointed to cortical networks DN-A and DN-B, but also to potentially additional networks associated with the intraparietal sulcus.<sup>37</sup> Therefore, in the current study, besides the cortical networks DN-A and DN-B, we also considered three additional cortical networks with known representations in the intraparietal sulcus - the parietal memory network<sup>44</sup> (also known as the salience network<sup>42,43</sup>; PMN/SAL) and two subdivisions of the canonical frontoparietal network<sup>46</sup> - frontoparietal network A (FPN-A) and frontoparietal network B (FPN-B).<sup>42,47</sup> The networks were validated using a surface-based correlation analysis with seeds positioned within the network boundaries defined by MS-HBM. All networks of interest in each participant are presented in Figure 1.

#### Entorhinal cortex and hippocampus masks: Volumetric data

For exploration of the cortical networks associated with the hippocampal-entorhinal system, we used spatial masks applied on processed volumetric data. For defining the hippocampus, we used participant-specific hippocampal segmentation derived from the *recon\_all* function implemented in FreeSurfer<sup>104</sup> (v7.01). In each participant, the hippocampal masks were cleaned of anatomically misplaced voxels. For defining the entorhinal cortex, we used the Oxford-Harvard cortical atlas mask covering the anterior segment of the cortical MTL and containing the entorhinal cortex, pre/parasubiculum and large parts of the perirhinal cortex. In each participant, voxels associated with the perirhinal cortex were removed. Manual segmentation of the entorhinal cortex in each participant was done based on anatomical landmarks defined by cytoarchitectonic delineations of the human entorhinal cortex and identified in each participant using their T1-weighted image.<sup>57,107–109</sup> Note that the resulting entorhinal cortex mask covered the entire anterior segment of the parahippocampal gyrus and therefore, included also the pre/parasubiculum (Figure S1).

### Functional connectivity analysis: Network associations in the MTL

For associating the individually defined cortical networks with the hippocampal-entorhinal system, we used independent exploration datasets comprising the remaining 24 fixation task runs (23 runs for P4), resulting in about three hours of BOLD data for each participant. The volumetric data were spatially smoothed using a 4 mm FWHM kernel.

First, we used individual cortical network boundaries derived from MS-HBM to calculate the average time-series for each network of interest. Next, we estimated Pearson correlation coefficients between the network-level time-series and the time-series of each voxel within the entorhinal cortex and hippocampus for each BOLD run. The resulting correlation coefficients were averaged across all available BOLD runs in the independent exploration datasets. These analysis steps resulted in an average Pearson correlation coefficient associating each cortical network of interest and each voxel in the entorhinal cortex and hippocampus.

To determine the cortical network that is preferably associated with each entorhinal cortex and hippocampus voxel, we used independent exploration datasets and a winner-takes-all approach<sup>40,41,51</sup> in which the network with the highest Pearson correlation coefficient with a given voxel was assigned to that voxel. Two following constraints were applied to the winner-takes-all procedure. First, we used a threshold of  $z(r) > 0.05$  to remove noisy voxels with low correlation values from the analysis. Second, mixed voxels with less than 5% difference in correlation values between cortical networks were removed as well from the analysis. Even though our dataset was specifically optimized for high data quality in the medial temporal lobe, the most lateral portions of the entorhinal cortex (delimited by the collateral sulcus) and the most anterior portions around the ambient gyrus still suffered from signal loss and dropout. Therefore, only cortical networks that showed consistent bilateral connectivity patterns across all four participants were used for the winner-takes-all procedure.

Note that there are some inherent limitations to the winner-takes-all approach. For example, both cortical networks DN-A and DN-B associated strongly with the medial band of the entorhinal cortex (Figure S4). However, cortical network DN-A associated with the voxels located at the medial band of the entorhinal cortex to a greater extent compared with the cortical network DN-B.

### Individualized gradient analysis

We used diffusion map embedding to recover a low-dimensional embedding from whole-brain connectivity data. For each participant, fixation task data were used to estimate a whole-brain cross-correlation matrix. For this purpose, Pearson correlation coefficients were calculated between each vertex and all the other vertices in the fsaverage6 space, resulting in a 40,962 x 40,962 cross-correlation matrix per hemisphere. The cross-correlation matrices were Fisher z-normalized, combined across hemispheres, averaged across all available data for each participant and subjected to diffusion map embedding (see Margulies et al.<sup>55</sup> for more details). Since in the current study we were interested in positioning the subregions of the human MTL on the unimodal-transmodal processing axis, we used only the principal gradient from the diffusion map embedding analysis.<sup>55</sup> To calculate the principal gradient values for the hippocampus, entorhinal cortex, perirhinal cortex, and the parahippocampal cortex, we averaged the gradient values for each cortical network that was associated with each of these MTL subregions.

### Two-dimensional entorhinal cortex maps

To display the cortical networks associated with the entorhinal cortex on a two-dimensional surface map, we used the cytoarchitectonic parcellation of the human entorhinal cortex previously reported in Insausti et al.<sup>57</sup> For each participant, eight coronal slices that sequentially followed the entorhinal cortex anterior-posterior axis beginning from the ambient gyrus (anterior entorhinal cortex in Figure 2; 2 mm gap between slices) were analyzed. Accordingly, the entorhinal cortex template posterior to the ambient gyrus (marked with a green dashed line in Figure 5B) was divided into eight slices. The slices and their approximate orientation were determined by data presented in Insausti et al.<sup>57</sup> In each participant, for each coronal slice, we mapped the cortical networks positioned on the surface voxels of the parahippocampal gyrus mask, interpolated across hemispheres, and projected each network's relative length on the corresponding slice in the two-dimensional entorhinal cortex template. Note that the entire surface of the parahippocampal gyrus mask (which included the entorhinal cortex and at least parts of the pre/parasubiculum) was assigned to the entorhinal cortex,

For the group level projection (Figure 5B), for each position on a coronal slice, we applied a winner-takes-all approach to determine the winning network across subjects. When the network assignment was split equally across subjects, the winning network was determined by the network identity in the previous slice. Since the entorhinal lateral band was found to be associated with at least two different networks, slices with equal distribution of networks were represented using a color gradient.

## QUANTIFICATION AND STATISTICAL ANALYSIS

In this study, four participants were scanned four times each, which resulted in 32 fixation task runs for each individual participant. For participant 4 one run was excluded due to excessive head movement (maximum absolute head displacement of 2.9 mm). For each participant, eight runs were used for defining distributed cortical networks using MS-HBM. Due to lower signal quality in the anterior and lateral parts of the entorhinal cortex, all remaining 24 runs (23 runs for participant 4) were used for exploring the associations between the selected cortical networks in the entorhinal cortex and the hippocampus. For statistical analyses we used paired t-tests with significance level set to  $p < 0.05$ . All bar graphs throughout the manuscript represent mean Fisher z-transformed Pearson correlation coefficients  $\pm$  SEM.